

PAPER • OPEN ACCESS

Thermosyphon assisted melting of PCM inside a rectangular enclosure: A synergistic numerical approach

To cite this article: R Srikanth *et al* 2016 *J. Phys.: Conf. Ser.* **745** 032130

View the [article online](#) for updates and enhancements.

Related content

- [Experimental study of stability and transients in a horizontally heated boiling helium thermosyphon](#)
H Furci, A Four and B Baudouy
- [Experiments and simulations on a thermosyphon solar collector with integrated storage](#)
P Toninelli, A Mariani and D Del Col
- [An Innovative Enhanced Wall to Reduce the Energy Demand in Buildings](#)
F Fantozzi, S Filipeschi, M Mameli et al.

Recent citations

- [Two-stage heat transfer characteristics of constrained melting inside an isothermally heated horizontal cylinder](#)
Zeshi Gao *et al*



IOP | ebooks™

Bringing together innovative digital publishing with leading authors from the global scientific community.

Start exploring the collection—download the first chapter of every title for free.

Thermosyphon assisted melting of PCM inside a rectangular enclosure :A synergistic numerical approach

Srikanth R ¹, Rohit S Nair ², C Balaji ³

^{1,2} Research scholar, Heat Transfer and Thermal Power Laboratory, Department of Mechanical Engineering Indian Institute of Technology Madras, Chennai 600036 , India

³ Professor, Heat Transfer and Thermal Power Laboratory, Department of Mechanical Engineering Indian Institute of Technology Madras, Chennai 600036 , India

E-mail: balaji@iitm.ac.in

Abstract. Melting of a phase change material assisted by a thermosyphon inside a two dimensional rectangular domain is numerically investigated. The PCM used is n-icosane and the thermosyphon is made of copper. The working fluid is water. The fill ratio of the working fluid (water) is taken to be 50 %. A lumped model is used for the simulation of transient operation of the thermosyphon and enthalpy-porosity method is employed for numerical simulation of melting of PCM. The effects of inclusion of multiple heat pipes on the melting of the PCM inside the enclosure is studied. Simulation results indicate that the addition of heat pipes enhances the performance of latent heat thermal energy storage system only upto a certain extent.

NOMENCLATURE

Greek symbols

α	Thermal diffusivity , m^2/s
β	Thermal expansion coefficient of PCM , K^{-1}
γ	melt fraction
ν	kinematic viscosity , m^2/s
ρ_s	Density, kg/m^3

Notations

a	length of the enclosure, mm
A_c	Surface area of the condenser section, m^2
C_f	thermal capacitance of the working fluid, kJ/K
C_w	thermal capacitance of the thermosyphon wall, kJ/K
c_p	specific heat at constant pressure, kJ/kgK
g	acceleration due to gravity, $9.81 m/s^2$
h	enthalpy, kJ/kg
h_e	heat transfer coefficient at the evaporator, W/m^2K
h_c	heat transfer coefficient at the condenser wall, W/m^2K
k	thermal conductivity, W/mK



L_c	length of the condenser, mm
L_e	length of the evaporator, mm
Nu	Nusselt number, non-dimensional heat transfer coefficient at the condenser wall
Q_e	Heat input to the evaporator, W
Q_{net}	net heat transfer, Sum of the axial heat and the boiling heat at any given time instant, W
Ra	Rayleigh number, dimensionless number associated with buoyancy-driven flow
S	heat pipe spacing, mm
S_e	inner surface area of the evaporator, mm^2
S_c	outer surface of the condenser, mm^2
t_c	thickness, mm
t_e	evaporator thickness, mm
T_{cond}	Condenser wall temperature, K
T_w	average evaporator wall temperature, K
T_{wat}	average PCM temperature, K
T_f	average fluid temperature, K

ABBREVIATIONS

<i>HP</i>	Heat pipe
<i>LHTES</i>	Latent heat thermal energy storage
<i>PCM</i>	Phase change material
<i>TCE</i>	Thermal Conductivity Enhancers

1. Introduction

Latent heat thermal energy storage systems (LHTES) that employ Phase change materials (PCMs) are considered to be one of the most efficient techniques to store energy. The main advantage of using a LHTES is their ability to store thermal energy with a minimal temperature change. However the low thermal conductivity of PCMs pose a great challenge to heat transfer experts owing to the difficulty in heat transport. Various techniques like fins, heat pipe have been adopted in conjunction with PCMs to enhance the thermal conductivity of the LHTES over the years. A thermosyphon is a gravity assisted wickless heat pipe containing a working fluid, which undergoes phase change during the transient operation of the heat pipe. The evaporator section of the heat pipe filled with water absorbs the major portion (>80%) of the heat input. The condensation at the condenser serves as the heat source for the PCM. Ho and Viskanta [1] reported the basic heat transfer data during melting from an isothermal vertical wall. n-octadecane was used as a PCM and cavity shape was rectangular. Shadowgraph technique was used to capture the position of the solid liquid interface position and a corresponding numerical model was also developed. Good agreement between the experiment and numerical simulation was found. Webb and Viskanta [2] attempted to determine the characteristic length scale for correlating melting heat transfer data from a vertical wall. They concluded that height of the enclosure should not be used as the characteristic length scale for melting heat transfer correlations. The authors also suggested the usage of length in the direction of temperature gradient as the characteristic length. Bejan [3] discussed the basic natural convection correlations from a vertical wall under isothermal boundary conditions. Voller and Prakash [4] developed a generalized methodology for the modeling of mushy region phase change problem. They concluded that the Darcy source terms and the latent heat source term are the driving parameters in the fixed grid modeling approach. The main objective of the study was to present an enthalpy formulation based fixed grid methodology for phase change problem with convection. Farsi et al. [5] experimentally studied the transient behavior of a two-phase thermosyphon. The authors also

developed an analytical model for the thermosyphon systems and a good agreement between the model and the experiment was seen.

Liu et al. [6], experimentally studied the heat transfer characteristics of a heat pipe with a LHTES during both the charging and the discharging cycles. The authors also performed a simplified thermal resistance analysis and matched the numerical results with those of experiments. Shabgard et al. [7] developed a thermal resistance model to analyze the high temperature LHTES. The authors analyzed the effect of insertion of multiple heat pipes in a PCM enclosure for solar applications and concluded that the addition of heat pipes enhanced the performance of LHTES. Robak et al.[8], experimentally investigated the enhancement in the performance of a latent heat storage system due to addition of heat pipes and fins. The performance of the heat pipe is evaluated during both charging and discharging cycles. The authors concluded that the melting rates are enhanced by 60 % by the inclusion of heat pipe over fins. Weng et al. [9], experimentally investigated the application of heat pipe with PCM for electronic cooling. The evaporator section of the heat pipe takes up the heat generated by the electronics and discharged through the condenser into the PCM. Three kinds of PCMs were investigated and the authors concluded that the use of tricosane as PCM proved to be more efficient for the heat pipe operation.

Wang et al. [10], experimentally investigated the melting process in the vicinity of a heated vertical wall inside a rectangular enclosure. The authors developed a correlation for the melt fraction with Fourier number (Fo), Nusselt number (Nu), Rayleigh number(Ra). Tiari et al. [11] numerically studied the effect of melting of high temperature PCM assisted by multiple finned heat pipes inside a square enclosure. The authors concluded that an increase in the number of HPs increased the charging cycle time of the LHTES. Furthermore they reported that the convection plays an important role during the melting process .Srikanth et al.[12] performed a geometric optimization on a PCM based composite heat sink with metallic fins as thermal conductivity enhancers (TCEs). The authors concluded that the spacing between the fins (TCEs) in all the three directions has a significant effect on both the charging and discharging cycle times. The authors stressed upon the fact that the spacing that favored the charging cycle, did not perform well during the discharging cycle.

From the review of literature it is very much evident that the heat pipe-PCM integrated energy storage systems research is a topic of serious research in the recent times. Furthermore, numerical simulations rarely capture the transient response of the heat pipe. Researchers modeled heat pipe as a high conducting copper rod and argued that addition of heat pipes increased the charging time. The main objective of this paper is to get to the bottom of the problem and numerically investigate the effects of heat pipe number/spacing on the melting of PCM over a wide range. Furthermore, this numerical study aims to capture the transient response of the heat pipe during the charging cycle which is scarce in the literature.

2. Physical model

A schematic view of the geometries investigated is shown in Fig 1. Five sets of geometry, with single and multiple HPs are modeled.

The heat pipes comprise an evaporator section and a condenser section and are made of copper. The length(L_e) and diameter (d_e)of the evaporator section are 30 and 50 mm respectively. The length(L_c) and diameter(d_c) of the condenser section are 60 and 50 mm respectively. The details of the cases studied are tabulated in Table 1.

The entire model is at an initial temperature of 300 K. The evaporator section of the heatpipe is supplied with a total heat input of 6 W. In model 1, the system is designed in such a way that the entire heat load is taken up by a central heat pipe and aids in the melting of PCM. In model 2, the system is designed in a way that the total heat load is shared by three heat pipes that are equally spaced. In model 3,4 and 5, the heat load is share by five, seven and nine heat

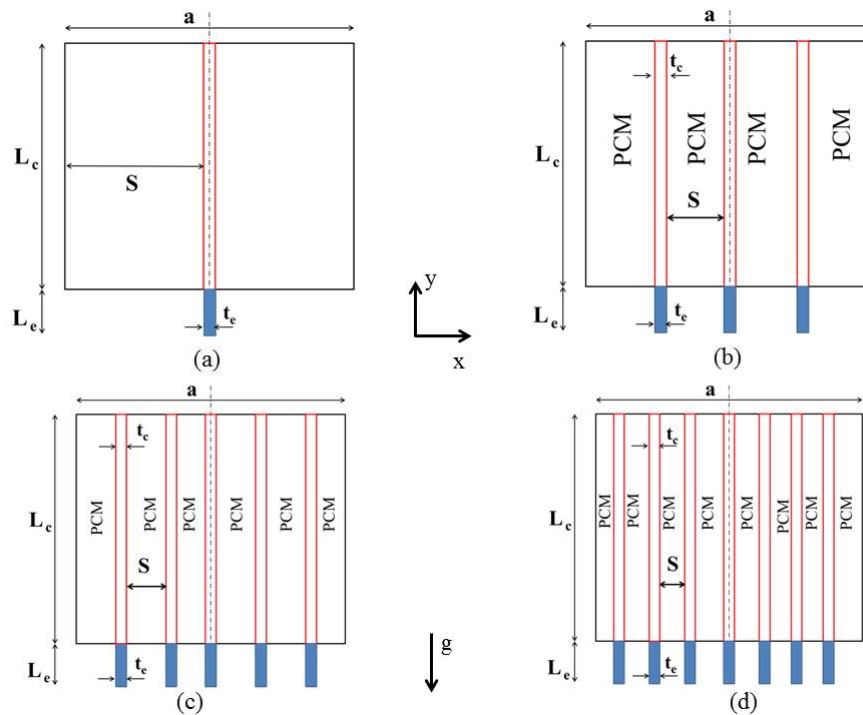


Figure 1. Model with (a)1 HP (b) 3 HP (c) 5 HP (d) 7 HP

Table 1. Model description

Model No	Number of HPs	Spacing (S), mm
1	1	27.5
2	3	11.25
3	5	5.75
4	7	3.125
5	9	1.5

pipes respectively. Hence, the addition of HPs essentially redistributes the total heat input.

3. Numerical procedure

3.1. PCM

The rectangular domain contains PCM and the heat pipe(HP) unit. The PCM used in this study is n-eicosane. The properties of the PCM is shown in Table 2. All properties of PCM were taken as constant regardless of the phase except for the specific heat whose values were measured at 50 temperature points in the range of 30 to 50 °C. In view of this a piecewise linear function for the variation of specific heat with temperature was assumed for the purpose of numerical study. At time $t=0$, temperature of 300K is assumed everywhere. The following assumptions were made during the CFD calculations

- n-eicosane is isotropic and homogeneous
- Laminar flow
- Boussinesq approximation is valid
- Liquid PCM is a Newtonian fluid

- Volumetric expansion of the PCM is negligible

Table 2. Properties of n-eicosane

Material	k, W/mK	C _p , kJ/kg K	hL kJ/kg	Melting point, C
n-eicosane	0.15	1.9	237.4	36.5

The governing equations for this problem [12] are the mass, momentum and the energy equations. The enthalpy-porosity technique is used to track the solid-liquid interface front of the PCM. In this method the temperature dependence of the energy equation is transformed into enthalpy dependence. The main advantage of using the enthalpy porosity model is that there is no explicit boundary condition needed at the solid-liquid interface. The inclusion of source term in the momentum equation allows for a gradual decrease in the fluid velocity, when the PCM changes from liquid to solid phase.

The continuity equation:

$$\frac{\partial \rho}{\partial t} + \rho(\nabla \cdot \mathbf{v}) = 0 \quad (1)$$

Momentum equations:

$$\frac{\partial \mathbf{v}}{\partial t} + \mathbf{v} \cdot \nabla \mathbf{v} = -\frac{1}{\rho} \nabla p + \nu \nabla^2 \mathbf{v} + \mathbf{g} + S_m \quad (2)$$

Energy equation:

$$\frac{\partial}{\partial t}(\rho h) + \nabla \cdot (\rho \mathbf{v} h) = \nabla \cdot (k \nabla \mathbf{T}) \quad (3)$$

The methodology is same as discussed in [4].

3.2. Heat pipe

The operation of the wickless heatpipe is modeled using a simplified lumped parameter model. Fig. 2 explains the nodalization of the lumped model

The following assumptions are used for the lumped modeling of wickless heatpipe

- One dimensional heat transfer
- Uniform heating and cooling
- Vapor and liquid inside the thermosyphon are at thermal equilibrium and hence at saturation state
- No axial heat losses
- Fluid thermal capacity is approximated as the liquid thermal capacity since vapour thermal capacity is negligible

The governing equations for the model are as follows

$$C_w \frac{\partial T_w}{\partial t} = Q_e - h_e S_e (T_w - T_f) \quad (4)$$

$$C_f \frac{\partial T_f}{\partial t} = h_e S_e (T_w - T_f) - h_c S_c (T_f - T_{wat}) \quad (5)$$

$$T_{cond} = T_{wat} + \frac{Q_{net}}{h_c \times A_c} \quad (6)$$

In this study h_e is the average evaporator heat transfer coefficient. - The nucleate boiling heat transfer coefficient is calculated from Froster-Zuber equation

3.3. Coupling

The lumped model discussed above is incorporated with Ansys Fluent as User Defined Function (UDF) subroutines . The condenser flux calculated by the UDF is applied as the input flux for the condenser section in the Enthalpy porosity model.

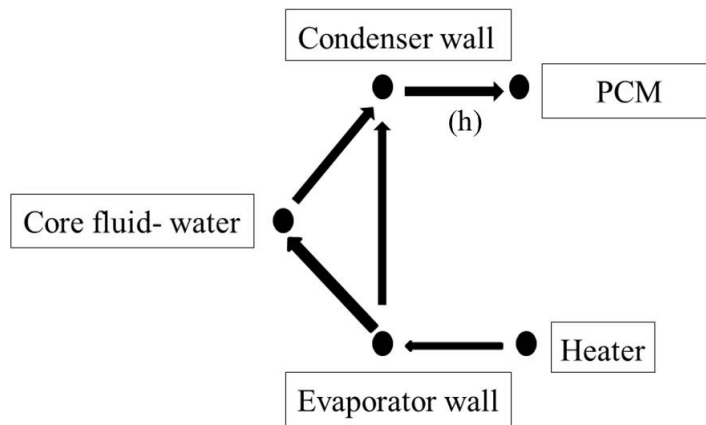


Figure 2. Nodal representation of the numerical model

The Nusselt number from the heated wall is calculated by using the following relation

$$Nu = \frac{h_c \times L_c}{k} \quad (7)$$

To account for the buoyancy effect inside the liquid PCM that drives the heat transfer, Rayleigh number is included in the study. The Rayleigh number is also defined [6] based on the PCM thickness.

$$Ra = \frac{g \beta \Delta T L_c^3}{\alpha \nu} \quad (8)$$

The heat transfer coefficient(h_c) at the condenser wall- PCM liquid interface is calculated based on a quasi -steady approach such that during each step the system proceeds through a sequence of quasi-steady states for dynamic equilibrium. The case of natural convection from a vertical wall-under constant heat flux at every time instant is used to calculate h_c . The following correlation is used for the calculation of the heat transfer coefficient for each step. From the iso heatflux condition on a vertical wall, the Nu and Ra can be correlated by using the wall averaged Nusselt number relation mentioned in chapter 5 of [3]

4. Validation

The enthalpy-porosity model and the lumped heat pipe model has been validated by experimental results available in literature. Experiments were conducted by [12] on a PCM basd heat sinks with pin fins. The numerical model was validated with the results of experiments and close match was found.

Furthermore, the heat pipe lumped model was validated with the experimental results of Farsi et al. [5]. as shown in Fig 3

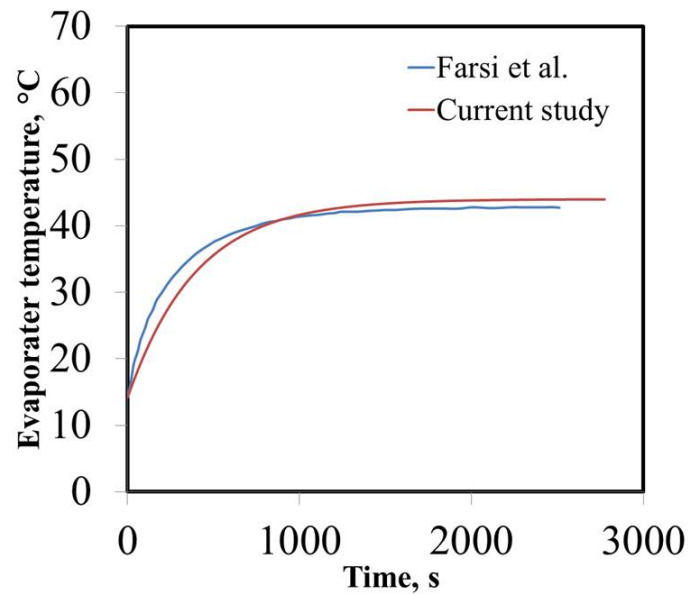


Figure 3. Comparison of temperature time history using the lumped model with the results of Farsi et al.

Commercially available Ansys Fluent 14.0 was used to solve the governing equations. Due to symmetry of temperature and flow fields with respect to y axis, the domain was modeled as symmetry, for each case, only one half of the entire geometry is considered with a symmetry boundary condition at the centrally placed HP axis.

Grid independence results indicated that a total of 100456 and 56768 elements was found sufficient for the 1HP case and 7 HP case respectively. A time step size of 0.05s was found sufficient as additional time size refinement did not enhance the accuracy of the computation. In order to improve the convergence stability in this study during the phase change process, the under relaxation factors of 0.5, 0.3 and 0.9 were considered for the momentum, pressure and melt fraction, respectively. Convergence residual values of 10^{-6} , 10^{-6} and 10^{-10} were set for continuity, momentum (x and y velocities) and energy equations, respectively. In each time step, the convergence criteria were achieved after 150 iterations.

5. Results and discussion

To evaluate the performance of LHTES, the following parameters and their transient variation are considered in this study

- condenser wall temperature
- PCM melt fraction
- Liquid PCM velocity
- condenser wall heat flux

For model 1 with single HP, there is a large thermal resistance setup between the heated wall (condenser) and the unmelted PCM zone. This results in high temperature of both the condenser and the evaporator wall. Initially the melt fraction of the PCM increases with time. The rate of melting gradually decreases with time when 5 % of the PCM is melted. This is due

to the fact that the PCM closer to the wall takes up all the thermal energy and forms a zone of high thermal resistance for the flow of heat.

The LHTES thermal conductivity can be enhanced by incorporating more HPs in the area experiencing high resistance for the flow of heat. Addition of HPs lead to a decrease in PCM mass in the system. Hence, an optimal value of HPs to the PCM in a LHTES system is always desired.

In model 2 and 3, as the number of HPs is increased (spacing is decreased) the charging process becomes fast as seen in Fig 4(a). In cases with lower spacing, the natural convection in the liquid PCM near the heated surface helps in transferring heat to the unmelted PCM zone. Hence, the growth of wall temperature is much slower in model 2 and 3. From this it is evident that the natural convection plays a significant role in the melting process.

The volume ratio v_h of the HPs can be defined as

$$v_h = \frac{\text{Amount of fin}}{\text{Amount of PCM}} \quad (9)$$

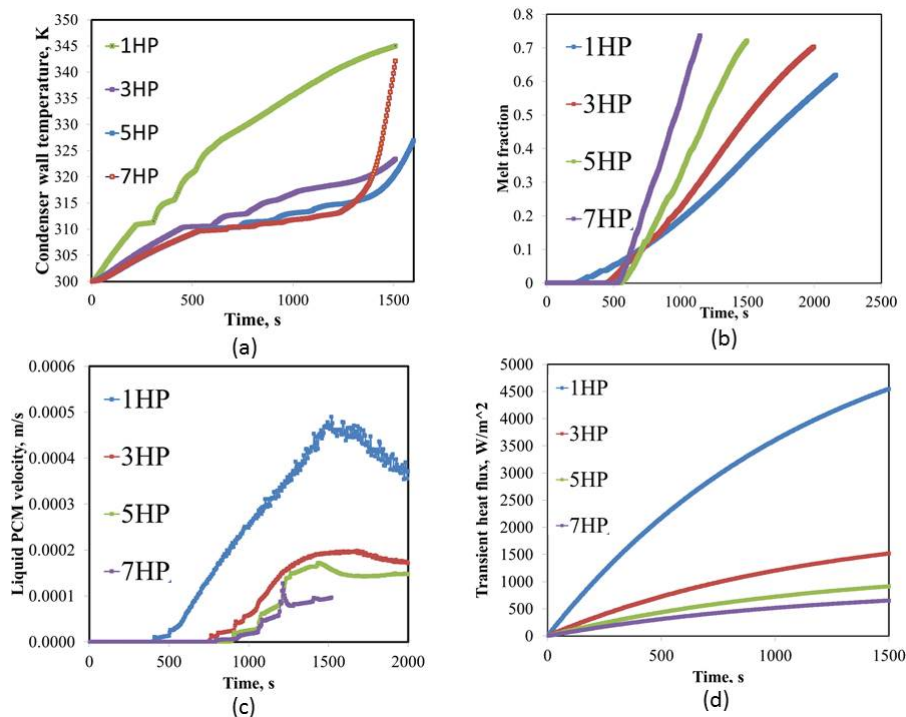


Figure 4. (a) Transient condenser wall temperature history for the 4 models (b) Transient melt fraction for the 4 models (c) Transient liquid PCM velocity history for the 4 models (d) Transient condenser wall heat flux history for the 4 models

Furthermore as the number of HPs is increased, the mass of the PCM in the system is reduced proportionally. It is intuitive that there exist an optimum ratio of HPs to the mass of the PCM for the best performance of LHTES.

For the cases with 3 and 5 HPs, the LHTES system provides high melt fraction and lower base wall temperature as seen in Fig. 4(a). This is a direct effect of the natural convection where the PCM layers receive heat from both the boundaries.

The condenser wall temperature is measured throughout the length of the condenser. The PCM velocity and mass fraction are calculated in the PCM module. The volume averaged parameters are taken for the PCM portion

Furthermore, from the transient history of melt fraction seen in Fig 4(b) for the four cases, it is evident that as the number of heat pipes is increased, the time to melt 70 % of PCM decreases monotonically. This is invariably due to the fact that the increase in HPs results in decrease of PCM mass. The transient variation of liquid PCM velocity and condenser wall heat flux are shown in Fig. 4(c) and 4(d) respectively. To evaluate the performance of the LHTES, the condenser wall temperature after 1500s of heating is monitored. Lower the wall temperature, results in better performance. As can be seen from Fig 4(a), the single HP case has the maximum temperature of 344K after 1500s of charging cycle. As the number of HPs is increased , the performance of LHTES systems becomes better.

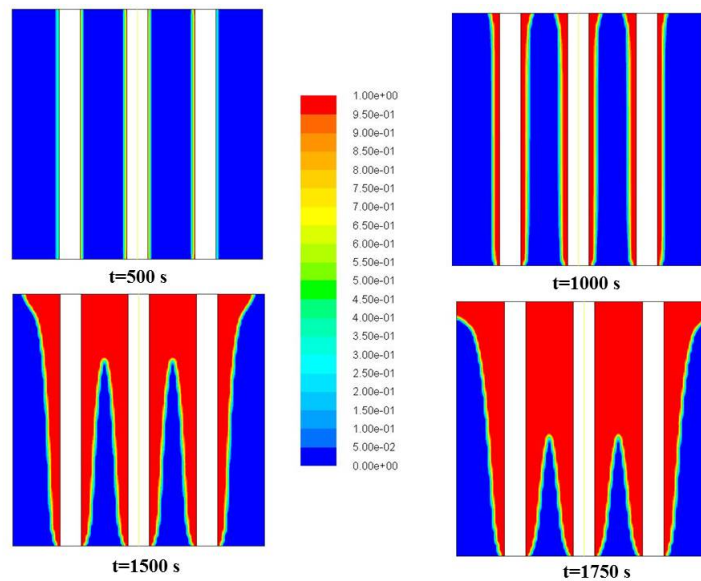


Figure 5. Contours of the volume fraction of the case with 3 HPs

For the 5 HP case the system is maintained at 319 K. An increase in heat pipe number beyond this, degrades the performance of the LHTES system (Indicated in bold face in Table 2). The temperature of the condenser wall shoots up to 330K. Hence caution needs to be exercised while designing the LHTES system to keep an optimum ratio of the volume HPs to the PCM to enhance the system performance

However, addition of HPs beyond a particular number has an adverse effect on the LHTES. Furthermore, from Table 3 it is evident that for models 2 and 3, after 1500s only 50 % and 70 % of the PCM have melted respectively. Natural convection plays a significant role in transfer of heat to the unmelted PCM in a uniform pattern. This effect is reflected in the velocity plot seen in Fig. 4(c), when the velocities are seen to be almost constant from t=1200 to 1600s for 3 Hp and 5 Hp cases. The melt fraction contours for the 3 HP case is shown in Fig.5

Table 3. Variation of temperature and melt fraction with increase in number of HPs

Model ID	Number of Hps	v_h	Temperature after 1500s (K)	Melt fraction after 1500s
1	1	0.26	345	0.38
2	3	0.79	323	0.50
3	5	1.31	319	0.72
4	7	1.83	339	0.89
5	9	2.36	360	1.00

The relatively constant velocity (Fig 4c) observed during the melting in case 5, contributes to the consistent heating of the solid PCM and shows up the best performance. The gradual erosion of the unmelted solid layer in 5 HP case helps maintain the condenser wall temperature below safe limit (usually 333 K)

6. Conclusions

The melting process of a thermosyphon assisted LHTES system with n-eicosane as PCM enclosed by a square enclosure was numerically simulated using a synergistic transient numerical approach, wherein a lumped model was combined with full numerical simulations. The effects of heat pipe spacing, numbers and the effect of natural convection on the melting process were studied. From the numerical study, it was evident that natural convection plays a significant role in the melting process of PCM. Furthermore, it was seen that there exist an optimum ratio of heat pipe volume to PCM volume that enhances the performance of LHTES system. Therefore, increasing the number of HPs maintain the LHTES system under safe limit only upto a particular number, and for the problem under consideration this number is 5.

References

- [1] Ho C J and Viskanta R 1984 *Journal of Heat Transfer* **106** 12–19
- [2] Webb B and Viskanta R 1985 *International Communications in Heat and Mass transfer* **12** 637–646
- [3] Bejan A 2013 *Convection heat transfer* (John Wiley, New York)
- [4] Voller V R and Prakash C 1987 *International Journal of Heat and Mass Transfer* **30** 1709–1719
- [5] Farsi H, Joly J L, Miscevic M, Platel V and Mazet N 2003 *Applied Thermal Engineering* **23** 1895–1912
- [6] Liu Z, Wang Z and Ma C 2006 *Energy Conversion and Management* **47** 967 – 991
- [7] Shabgard H, Bergman T, Sharifi N and Faghri A 2010 *International Journal of Heat and Mass Transfer* **53** 2979 – 2988
- [8] Robak C W, Bergman T L and Faghri A 2011 *International Journal of Heat and Mass Transfer* **54** 3476 – 3484
- [9] Weng Y C, Cho H P, Chang C C and Chen S L 2011 *Applied Energy* **88** 1825–1833
- [10] Wang Y, Amiri A and Vafai K 1999 *International Journal of Heat and Mass Transfer* **42** 3659–3672
- [11] Tiari S, Qiu S and Mahdavi M 2015 *Energy Conversion and Management* **89** 833–842
- [12] Srikanth R, Nemani P and Balaji C 2015 *Applied Energy* **156** 703–714